

# Quantum Oscillations in the Zeroth Landau Level: Serpentine Landau Fan and the Chiral Anomaly

T. Devakul<sup>1,2</sup>, Yves H. Kwan,<sup>3</sup> S. L. Sondhi,<sup>2</sup> and S. A. Parameswaran<sup>3</sup>

<sup>1</sup>*Department of Physics, Massachusetts Institute of Technology, Cambridge, Massachusetts 02139, USA*

<sup>2</sup>*Department of Physics, Princeton University, Princeton, New Jersey 08540, USA*

<sup>3</sup>*Rudolf Peierls Centre for Theoretical Physics, Clarendon Laboratory, Oxford OX1 3PU, United Kingdom*

 (Received 19 March 2021; revised 17 June 2021; accepted 5 August 2021; published 9 September 2021)

We identify an unusual mechanism for quantum oscillations in nodal semimetals, driven by a *single* pair of Landau levels periodically closing their gap at the Fermi energy as a magnetic field is varied. These “zero Landau level” quantum oscillations (ZQOs) appear in the nodal limit where the zero-field Fermi volume vanishes and have distinctive periodicity and temperature dependence. We link the Landau spectrum of a two-dimensional (2D) nodal semimetal to the Rabi model, and show by exact solution that, across the entire Landau fan, pairs of opposite-parity Landau levels are intertwined in a “serpentine” manner. We propose 2D surfaces of topological crystalline insulators as natural settings for ZQOs. In certain 3D nodal semimetals, ZQOs lead to oscillations of anomaly physics. We propose a transport measurement capable of observing such oscillations, which we demonstrate numerically.

DOI: 10.1103/PhysRevLett.127.116602

*Introduction.*—Quantum oscillations (QOs)—the periodic modulation of transport [1] and thermodynamic [2] properties of materials as an external magnetic field  $\mathbf{B}$  is varied—are among the most striking manifestations of quantum mechanics in the solid state. The oscillation period depends on the shape of the Fermi surface (FS), while information on FS parameters and scattering mechanisms can be extracted from the oscillation amplitude and its temperature dependence [3]. The utility of QOs as a probe of electronic structure rests on two theoretical pillars. The first is Onsager’s result [4],

$$\Delta_{1/B}^O = 2\pi\mathcal{S}_e^{-1}, \quad (1)$$

relating their periodicity in  $1/B$  to an extremal cross-sectional FS area  $\mathcal{S}_e$  in a plane normal to  $\mathbf{B}$  (we set  $\hbar = e = 1$ ). The second is the Lifshitz-Kosevich formula [5]

$$R_{\text{LK}}(T) = \frac{2\pi^2 T}{\omega_c \sinh(2\pi^2 T/\omega_c)} \quad (2)$$

with  $k_B = 1$ , relating the temperature ( $T$ ) dependence of the oscillation amplitude (shown here for the first harmonic) to the cyclotron frequency  $\omega_c = B/m^*$ , allowing the extraction of the effective mass  $m^*$ , averaged over  $\mathcal{S}_e$ .

Topological insulators and nodal semimetals [6] modify this picture. The effective-mass approximation implicitly assumed in (1) and (2) is violated by Weyl or Dirac dispersions, and the QO phase is altered by electronic Berry phases of topologically nontrivial bands [7]. Although many features may be captured by adapting

the semiclassical theory [8,9], the latter assumes the existence of a FS at  $\mathbf{B} = 0$ . It does not readily apply if a FS is absent, as in an insulator, or when it shrinks to a point in two dimensions or a point or line in 3D, situations that cannot be generated solely by the intersection of unhybridized bands. Such systems enter the quantum limit for any  $\mathbf{B} \neq 0$ , necessitating a full solution of the Landau level (LL) spectrum.

In 2D, our focus in much of this Letter, a linear crossing of a pair of energy bands at  $E = 0$  is generically described by the 2D Dirac equation. Viewed in isolation, such a dispersion gives rise to a fan of LLs whose energies evolve  $\propto \sqrt{B}$ , with the exception of a single  $\mathbf{B}$ -independent LL at  $E = 0$ . While  $1/B$ -periodic QOs emerge at any finite doping, at charge neutrality—corresponding to a point-node FS for  $\mathbf{B} \rightarrow 0$ —conventional QOs are absent since no LLs cross the Fermi energy at  $E_F = 0$ . However, in bulk systems, such nodal points always appear in pairs that are usually separated in the Brillouin zone (BZ) for symmetry reasons. Consequently, in principle, there is always mixing of LLs emerging from distinct nodes. The intuitive expectation is that, as  $B$  is increased, the zero-energy LLs from distinct nodes will experience increasingly strong mutual level repulsion, pushing them away from  $E_F$  without intersecting it [10–13].

Here, we show that a class of nodal-point semimetals violates this expectation: the zero-energy LLs oscillate about each other in energy as  $B$  is varied, leading to robust QOs as they repeatedly intersect  $E_F$ . The simplest instance of this general phenomenon of zero-LL QOs (ZQOs) occurs when a pair of 2D parabolic bands with effective

mass  $m$  undergo a band inversion of strength  $\Delta$ . This leads to a degenerate nodal ring at  $|\mathbf{k}| = k_0 \equiv \sqrt{m\Delta}$ , which, assuming inversion or mirror symmetry, is generically gapped by hybridization except at a pair of nodal points at  $\pm\mathbf{k}_0 = \pm k_0 \hat{\mathbf{x}}$  with anisotropic velocities  $v_x = v_c \equiv \sqrt{\Delta/m}$ ,  $v_y = v$ . We relate the associated LL problem to the Rabi model of quantum optics and, by exact solution, identify a sequence of QOs at charge neutrality. Although  $S_e = 0$ , these zero-LL QOs show  $1/B$  periodicity controlled by the FS area  $S_0 = \pi k_0^2$  of the unhybridized bands at  $E_F = 0$ , corrected by a factor

$$\Delta_{1/B}^{\text{ZLL}} = 2\pi\gamma^2 S_0^{-1}, \quad \gamma = 1/\sqrt{1 - v^2/v_c^2}. \quad (3)$$

The ZQOs only occur if  $v < v_c$  and disappear above  $B_0 = S_0/\pi\gamma^2$ . They originate from the serpentine motion of two LLs that straddle  $E_F$  and periodically open and close their gap while remaining bounded within an envelope  $\mathcal{E}(B)$  and separated from other LLs. At temperatures where these two states dominate the spectrum, ZQOs show non-Lifshitz-Kosevich (LK) behavior

$$R_{\text{ZLL}}(T) = \frac{\mathcal{E}(B)}{2T} \tanh^2 \frac{\mathcal{E}(B)}{2T}. \quad (4)$$

The explicit form of  $\mathcal{E}(B)$ , given below, cannot be modeled by a cyclotron frequency with an effective mass, and as  $B \rightarrow 0$  has the nonperturbative form  $\mathcal{E}(B) \sim e^{-B^*/B}$ .

ZQOs differ from other proposed routes to QOs at  $S_e = 0$ . The purely orbital origin of ZQOs and the associated serpentine Landau fan distinguishes their mechanism from recent proposals of Zeeman-driven ‘‘LL inversions’’ [14]. As they do not invoke surface states stemming from a topologically nontrivial band structure, ZQOs differ from Fermi-arc QOs in Weyl or Dirac semimetal slabs [15]. The  $e^{-B^*/B}$  dependence of the ZQO envelope and their link to the unhybridized FS area are reminiscent of QOs in narrow-gap insulators [16–27]. Both phenomena can be understood by extending the semiclassical approach to include phase-coherent tunneling through classically forbidden regions in the BZ. However, the serpentine fan, the  $\gamma$ -dependent period, and the gap closings at  $E_F$  are special to ZQOs. Unlike QOs in insulators, whose effect on the conductivity is suppressed by the activation gap, ZQOs remain observable in transport even as  $T \rightarrow 0$ . ZQOs thus represent a distinct class of magnetic oscillation phenomenon.

Below, we substantiate these claims by introducing and exactly solving a model that exhibits ZQOs, derive (3) and (4), and explain their connection to the serpentine structure across the Landau fan. We argue that key features persist even upon relaxing simplifying assumptions of the solvable limit. We close with a discussion of the observability and interpretation of ZQOs.

*Model and LL spectrum.*—As noted above, the simplest model showing ZQOs begins with a  $kp$  Hamiltonian for a spinless band-inverted electron in 2D,

$$H(\mathbf{k}) = \left( \frac{|\mathbf{k}|^2}{2m} - \frac{\Delta}{2} \right) \tau^z + vk_y \tau^y, \quad (5)$$

where  $\Delta, v > 0$ , and  $\tau^\alpha$  are Pauli matrices acting in orbital space. At half filling and low energy, this yields the advertised Dirac cones at  $\pm\mathbf{k}_0$ , with anisotropic velocities  $(v_x, v_y) = (v_c, v)$ ; we present results in terms of  $k_0, v, v_c$ . The Dirac points are protected by inversion (parity)  $\mathcal{P}: \tau^z \otimes (\mathbf{k} \rightarrow -\mathbf{k})$  and time reversal  $T: K \otimes (\mathbf{k} \rightarrow -\mathbf{k})$ , where  $K$  is complex conjugation.

We incorporate a magnetic field  $B\hat{z} = \nabla \times \mathbf{A}$  via Peierls substitution  $\mathbf{k} \rightarrow \boldsymbol{\pi} = \mathbf{k} - \mathbf{A}$ , so that  $[\pi_x, \pi_y] = iB$ . We first obtain the LL spectrum numerically (Fig. 1), by truncating in the basis defined by  $a^\dagger a|n\rangle = n|n\rangle$ , where  $a = (\pi_x + i\pi_y)/\sqrt{2B}$  and  $[a, a^\dagger] = 1$  at large finite  $n$ . At small  $B$ , the low-energy spectrum has the Dirac LL form  $E_n \sim \sqrt{Bn}$ . As  $B$  is increased, pairs of LLs oscillate about each other in a serpentine manner, becoming degenerate at a series of crossing points absent for  $v > v_c$ . All crossings occur at a set of ‘‘magic fields,’’

$$B_N = \frac{m(\Delta - mv^2)}{2N + 1} = \frac{1}{\pi\gamma^2} \frac{S_0}{(2N + 1)}, \quad N = 0, 1, \dots, \quad (6)$$

whence we obtain (3). The final set of crossings occurs at  $B_0 = k_0^2/\gamma^2$ , beyond which  $E_n \sim Bn$  as for the unhybridized bands. The central pair of LLs that oscillate about  $E = 0$  are well separated from other LLs.

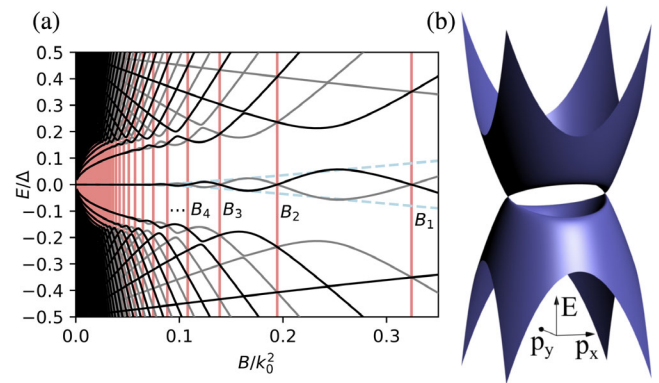


FIG. 1. (a) Serpentine Landau level fan computed for  $v = v_c/6$ . Even- and odd-parity LLs (black and gray lines) repeatedly self-intersect within a widening envelope as  $B$  is varied. ZQOs originate from a pair that repeatedly intersects the Fermi energy ( $E = 0$ ) at magic fields  $B_N$  (red lines), where the LL problem simplifies. The oscillation magnitude is well approximated by  $\pm\mathcal{E}(B)$  derived in the main text (dashed lines). (b) Zero-field dispersion of  $H$  (5).

In a rotated Pauli basis  $\sigma^\alpha = e^{(i\pi\tau^y/4)}\tau^\alpha e^{-(i\pi\tau^y/4)}$ , we have

$$H = \left( \frac{|\boldsymbol{\pi}|^2}{2m} - \frac{\Delta}{2} \right) \sigma^x + v\pi_y \sigma^y = \begin{pmatrix} 0 & h^\dagger \\ h & 0 \end{pmatrix}, \quad (7)$$

where  $h$  is the non-Hermitian Hamiltonian for a 1D harmonic oscillator in a constant imaginary vector potential,

$$h = \omega[a^\dagger a - \delta + \eta(a - a^\dagger)] \equiv \omega(A_+^\dagger A_- - \Gamma), \quad (8)$$

with  $\omega = (Bv_c/k_0)$ ,  $\delta = (k_0^2/2B) - \frac{1}{2}$ ,  $\eta = (v/v_c)(k_0/\sqrt{2B})$ , and  $\Gamma = (k_0^2/2\gamma^2 B) - \frac{1}{2}$ . The shifted ladder operators  $A_\pm = a \pm \eta$  are related to  $a$  via a similarity transformation by  $W = W^\dagger = e^{\eta(a+a^\dagger)}$ ,

$$A_+^\dagger = Wa^\dagger W^{-1}, \quad A_- = WaW^{-1}. \quad (9)$$

$h$  is diagonalized by right and left eigenvectors  $|w_n\rangle = W|n\rangle$  and  $\langle\bar{w}_n| = \langle n|W^{-1}$  with eigenvalues  $\lambda_n = \omega(n - \Gamma)$ , that are biorthogonal:  $\langle\bar{w}_n|w_{n'}\rangle = \delta_{nn'}$ . We observe that if  $h^\dagger h|\phi_i\rangle = E_i^2|\phi_i\rangle$  with  $E_i \neq 0$ , then the states  $|\psi_{i,\pm}\rangle = (|\phi_i\rangle, \pm(h/E_i)|\phi_i\rangle)$  are eigenstates of  $H$  with eigenvalues  $\pm E_i$ . Since the parity operator  $\mathcal{P} = (-1)^{a^\dagger a} \sigma^x \equiv P_a \sigma^x$  commutes with  $H$ ,  $\mathcal{P}|\psi_{i,\pm}\rangle = [\pm P_a(h/E_i)|\phi_i\rangle, P_a|\phi_i\rangle)$  is also an eigenvector of  $H$  with eigenvalue  $\pm E_i$ . For generic  $B \neq B_N$ ,  $\mathcal{P}$  does not enforce any degeneracies, and there are no  $E = 0$  solutions.

At magic fields  $B = B_N > 0$ , which exist only if  $v < v_c$ , additional structure emerges. First,  $\Gamma = N$ , so that  $|\psi_0\rangle = (|\phi_0\rangle, 0)$  and  $|\bar{\psi}_0\rangle = (0, |\bar{\phi}_0\rangle)$ , where

$$|\phi_0\rangle = \mathcal{N}_N^{-\frac{1}{2}}|w_N\rangle, \quad |\bar{\phi}_0\rangle = \mathcal{N}_N^{-\frac{1}{2}}|\bar{w}_N\rangle, \quad (10)$$

with  $\mathcal{N}_N = \langle w_N|w_N\rangle$ , are exact  $E = 0$  eigenstates of  $H$ . Furthermore,  $h^\dagger h$  only mixes  $|w_n\rangle$  with  $|w_{n\pm 1}\rangle$  and annihilates  $|w_N\rangle$  and hence has a decoupled subspace spanned by  $\{|w_{n \leq N}\rangle\}$ . Apart from the zero-energy states, this gives rise to  $2N$  energy levels  $|\psi_{i,\pm}\rangle$ ,  $i = 1, 2, \dots, N$  with  $|E_i| \neq 0$  expressible in terms of a finite sum of  $|w_n\rangle$ , via  $|\phi_i\rangle = \sum_{n=0}^N \phi_{i,n}|w_n\rangle$ . We now observe that  $P_a h = h^\dagger P_a$ ,  $P_a W P_a = W^{-1}$ , and hence  $P_a|w_n\rangle = (-1)^n|\bar{w}_n\rangle$ ; therefore,  $P_a h|\phi_i\rangle = h^\dagger P_a|\phi_i\rangle \equiv \sum_{n=0}^N \bar{\phi}_{i,n}|\bar{w}_n\rangle$  is a finite sum of  $|\bar{w}_n\rangle$ . This forces  $|\phi_i\rangle$  and  $P_a h|\phi_i\rangle$  to be linearly independent [28]: this follows since linear dependence requires  $\langle\bar{w}_m|P_a h|\phi_i\rangle \propto \langle\bar{w}_m|\phi_i\rangle = 0$  for  $m > N$  (due to biorthogonality), but since  $\langle\bar{w}_m|\bar{w}_n\rangle \neq 0$  generically, this over-constrains the  $\bar{\phi}_{i,n}$  and forces them to vanish, leading to a contradiction. Since  $|\phi_i\rangle$  and  $P_a h|\phi_i\rangle$  are linearly independent, so are  $|\psi_{i,\pm}\rangle$  and  $\mathcal{P}|\psi_{i,\pm}\rangle$ . Thus, each  $\pm E_i$  level is twofold degenerate, with orthogonal eigenstates obtained by projecting  $|\psi_{i,\pm}\rangle$  onto the even- and odd-parity sectors; including the  $E = 0$  states, there are thus  $2N + 1$  pairwise

LL crossings at  $B_N$ . As  $B$  is increased above  $B_N$ , the LLs split linearly with same-parity LLs from adjacent energies approaching each other and undergoing avoided crossings. The  $2N - 1$  LL pairs closest to  $E = 0$  again show crossings at  $B_{N-1}$ . The LLs thus oscillate about each other, forming serpentine pairs whose final crossing occurs at successively lower  $B$  for increasing  $|E|$  (Fig. 1). Since this structure relies on repulsion between adjacent LL pairs, it cannot be obtained by working perturbatively within each pair. The crossings are all observed to occur within the band overlap window  $|E| < \Delta/2$  and are a manifestation of the crossover between the distinct LL structures of the Dirac points and the parabolic band inversions. For  $v > v_c$ ,  $\Gamma < 0$  for all  $B$  and so there are no magic fields, and the serpentine structure is lost.

We can link the unusual structure of  $H$  to its membership in a class of quasi-exactly-solvable models [32]. Specifically, it can be mapped to an ‘‘analytic continuation’’ of the Rabi model [28], which is known to have rich analytical structure [33,34]. Finally, we discuss the effect of various perturbations on ZQOs in the Supplemental Material [28].

*Energy envelope.*—We estimate the ZQO envelope using perturbation theory near  $B_N$ , yielding definite-parity eigenstates  $(1/\sqrt{2})(|\psi_0\rangle \pm |\bar{\psi}_0\rangle)$  with approximate energies

$$E_\pm(B) \approx \pm \mathcal{E}(B) \cos(\pi B_0/2B) \quad (11)$$

to  $O(|B - B_N|^2)$  near any  $B_N$ , where  $\mathcal{E}(B_N) = B_N v_c / (\pi k_0 \mathcal{N}_N)$  is analytically continued to all  $B$ , and  $\mathcal{N}_n = e^{-2n^2} {}_1F_1(1 + n; 1; 4n^2)$  with  ${}_1F_1$  the hypergeometric function. Asymptotically, for  $B \ll B_0$  we have

$$\mathcal{E}(B) \approx \begin{cases} Bv_c / [\pi k_0 I_0(B'/B)], & B \ll (\gamma^2 - 1)B_0 \\ \sqrt{4Bv_c/\pi} e^{-B^*/B}, & B \ll (\gamma^2 - 1)B_0, \end{cases} \quad (12)$$

where  $I_0(x)$  is a Bessel function,  $B' = 2B_0\sqrt{\gamma^2 - 1}$ , and  $B^* = B_0\{\gamma\sqrt{\gamma^2 - 1} - \log(\gamma - \sqrt{\gamma^2 - 1})\}$  [28]. ZQOs depend exponentially on  $B$  for  $B \ll B'$  and saturate for  $B > B'$ . For  $v \ll v_c$ ,  $B' < B_0$  so there is a finite window where ZQOs are especially amenable to detection (though they are likely observable even in the exponential regime, which describes the entirety of Fig. 1). As  $v$  increases, this window shrinks, vanishing at  $v = v_c/\sqrt{5}$  when  $B' = B_0$ . For  $v_c/\sqrt{5} \leq v < v_c$ , ZQOs are always in the exponential regime and are absent for  $v \geq v_c$ . The exponential onset in  $B$  is a signature of ZQOs.

*Non-LK temperature dependence.*—Since ZQOs arise from the motion of just two states, we expect distinctive thermodynamic signatures at charge neutrality and low but finite temperature  $T = \beta^{-1}$ , controlled by the low-energy density of states per unit area [18]

$$D_\beta(B) = - \int dE n'_F(E) \rho(E) \approx \frac{\beta B / (4\pi)}{\cosh[\beta E_\pm(B) / 2]^2}, \quad (13)$$

where  $n'_F(E) = -\beta e^{\beta E} / (1 + e^{\beta E})^2$  is the derivative of the Fermi function,  $\rho$  is the single particle density of states, and we have taken into account the LL degeneracy per unit area  $B/2\pi$ . The final form is valid at temperatures where only the two central states  $E_\pm(B)$  contribute and leads to the non-LK behavior (4) in the oscillation magnitude. In the metallic limit  $v = 0$ , or at very high temperatures, the central two states can no longer be treated as separate from the remaining spectrum and the conventional LK form (2) is restored.

*Topological crystalline insulators.*—Having explained the origin of ZQOs in a solvable model and argued that they survive on relaxing its simplifying assumptions (and in the tight-binding limit [28]), we now turn to identifying experimental settings where they may be observable. Although the models discussed thus far are quite fine-tuned for quasiexact solvability, the physics of ZQOs should be relatively universal in Dirac systems with weakly gapped nodal rings. As a concrete example, consider the 2D surface of a 3D topological crystalline insulator [35] (TCI) with mirror symmetry (a description that encompasses the SnTe material class), described by the  $kp$  Hamiltonian [36]

$$H_T = v_T(k_x s^y - k_y s^x) + m_T \tau^x + \delta_T s^x \tau^y. \quad (14)$$

Although very different from  $H$ , the low-energy dispersion of  $H_T$  also hosts two Dirac cones connected via a weakly gapped nodal ring [37]. The positions of the two nodal points and their velocities are  $k_0 = \sqrt{\delta_T^2 + m_T^2} / v_T$ ,  $v_x = v_T$ ,  $v_y = \delta_T / k_0$ . The zero-energy eigenstates of  $H_T$  can be determined exactly and appear at fields  $B_{T,N} = m_T^2 / (2v_T^2 N)$  for positive integers  $N$ . The oscillation magnitude  $\mathcal{E}_T(B)$  displays the same qualitative behavior as  $\mathcal{E}(B)$  [28]. The parameters of  $H_T$  have been experimentally determined in a number of materials [36,39–42]. ZQOs occur for  $B < B_{T,1}$ , and depend exponentially on inverse field when  $B \ll B'_T = 2\delta_T m_T / v_T^2$ , from (12). As a typical example, parameters relevant to SnTe [36,39] give  $(B'_T, B_{T,1}) \approx (54, 52)$  T with the envelope function  $\mathcal{E}_T(15 \text{ T}) \approx 1$  K [28]. This places the corresponding ZQOs in the exponential regime and are observable within the ranges of fields and temperatures currently achievable in experiments using pulsed magnetic fields [43]. The parameters  $m_T$  and  $\delta_T$  are tunable by strain [38]: even a small change can have a significant effect on the ZQOs due to the exponential dependence. ZQOs can therefore serve as a sensitive probe of TCI surface states.

*Three dimensions.*—The physics of ZQOs also generalizes to 3D. A prototypical model for a Weyl semimetal with broken  $\mathcal{T}$  symmetry [6],

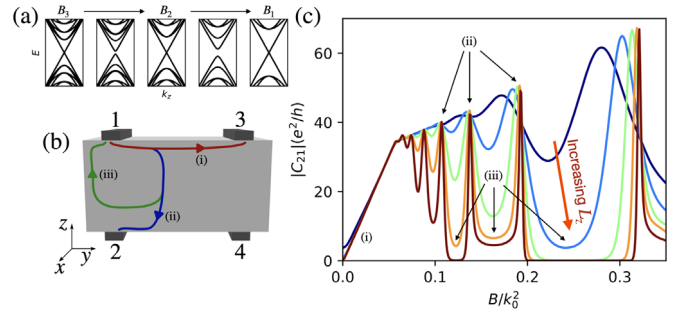


FIG. 2. (a) The LL dispersion of  $H_{\text{Weyl}}$  at and in between magic fields  $B_3$ ,  $B_2$ , and  $B_1$  for  $v = v_c/6$ , illustrating the  $1/B$ -periodic gap closings of the chiral LLs resulting from ZQOs. (b) A proposed experimental setup for observing ZQOs in 3D. Four leads are attached to a bulk Weyl semimetal. (c) Numerical results for the  $C_{21}$  element of the conductance matrix shows clear peaks at the magic fields.

$$H_{\text{Weyl}}(\mathbf{k}) = \left( \frac{|\mathbf{k}|^2}{2m} - \frac{\Delta}{2} \right) \sigma^x + vk_y \sigma^y + wk_z \sigma^z, \quad (15)$$

coincides with (5) (up to a mass term) at each  $k_z$  and therefore exhibits ZQOs under a magnetic field  $B\hat{z}$  for  $v < v_c$ . The condition  $v < v_c$  is naturally satisfied in Weyl semimetals that are proximate to a nodal line semimetal limit  $v = 0$  where the two nodes form a nodal ring, for example, in scenarios where the protecting symmetries of the Weyl ring are weakly broken [44,45]. The presence of zero modes at  $k_z = 0$  in a magnetic field corresponds to the existence of gapless bulk chiral LLs that propagate along  $\pm\hat{z}$ . Hence, ZQOs correspond to a periodic opening and vanishing of the gap between these chiral LLs, as illustrated in Fig. 2(a). Since gaplessness of these LLs is crucial to magnetotransport effects linked to the chiral anomaly and Fermi arcs [15,46–49], a striking implication of ZQOs is that such phenomena will also experience  $1/B$ -periodic revivals. As a demonstration, Fig. 2(b) shows a transport measurement capable of probing ZQOs: four leads labeled by  $i = 1, \dots, 4$  are connected to a bulk sample and the conductance matrix  $C_{ij}$ , defined in terms of the lead current and voltage via  $I_i = C_{ij}V_j$ , is measured. Figure 2(c) shows that  $C_{21}$ , computed numerically at  $T = 0$  for a discretized model, is highly sensitive to ZQOs and can be understood as follows. At zero and low fields, electrons from lead 1 flow mainly into Fermi-arc surface states, which drives current  $1 \rightarrow 3$  as indicated by (i). At higher fields, electrons are transferred to the bulk chiral modes before making it to lead 3 [15]. When these chiral modes are perfect (i.e., gapless at  $B = B_N$ ), electrons fully traverse the bulk and drives current  $1 \rightarrow 2$  (ii). Otherwise, electrons are only able to traverse a finite distance into the bulk before turning back, resulting in no current (iii). Indeed,  $C_{21}$  demonstrates clear peaks at each magic field, which become sharper with increasing thickness  $L_z$ . Details and discussion of the

numerical calculation, performed using the KWANT [50] code, is available in the Supplemental Material [28].

*Conclusions.*—In closing, we note a complementary perspective on ZQOs in the  $B \rightarrow 0$  limit emerges upon considering  $E = 0$  semiclassical tunneling trajectories in the BZ between the Dirac points at  $\pm k_0$ . These capture instanton events that generate repulsion between the zero-energy LLs of the Dirac points; they have a complex action, leading to a tunneling matrix element whose phase (amplitude) depends on  $\pi B_0$  ( $B^*$ ). Summing over tunneling events [51] and recalling that  $B$  plays the role of  $\hbar$  in the semiclassical expansion yields a result consistent with the  $B \rightarrow 0$  limit of (11). Intuitively, ZQOs emerge when optimal tunneling trajectories linking distinct  $B = 0$  Dirac points in the BZ involve an excursion to  $k_y \neq 0$  acquiring an Aharonov-Bohm phase and its associated interference effects, which vanish for  $v \geq v_c$  when these trajectories are fixed at  $k_y = 0$ . (Similar considerations yield QOs in narrow-gap insulators, but since these lack zero-energy LLs, it is more natural to view semiclassical effects as modulating the LL gap at  $E_F$  rather than generating LL repulsion.) This places ZQOs on conceptually similar footing with “tunneling interference” effects [52–57] and indicates that these ideas are broadly applicable. Finally, as a quasi-exactly-solvable model amenable to semiclassics, (5) is potentially noteworthy in the context of “resurgent asymptotics” in quantum mechanics [58–61].

We thank B. Assaf, B. A. Bernevig, A. I. Coldea, F. H. L. Essler, and L. Fu for discussions. We are especially grateful to N. Cooper for clarifying aspects of [16,17] and for a stimulating conversation on semiclassical trajectories in quantum oscillations. We acknowledge support from the European Research Council under the European Union Horizon 2020 Research and Innovation Programme, Grant Agreement No. 804213-TMCS (Y. H. K., S. A. P.). Additional support was provided by the Gordon and Betty Moore Foundation through Grant No. GBMF8685 toward the Princeton theory program.

---

[1] L. Shubnikov and W. J. de Haas, Proc. Natl. Acad. Sci. U.S.A. **33**, 130 (1930).  
 [2] W. J. de Haas and P. M. van Alphen, Proc. Natl. Acad. Sci. U.S.A. **33**, 1106 (1930).  
 [3] D. Shoenberg, *Magnetic Oscillations in Metals*, Cambridge Monographs on Physics (Cambridge University Press, Cambridge, England, 1984).  
 [4] L. Onsager, *Philos. Mag.* **43**, 1006 (1952).  
 [5] L. Lifshitz and A. Kosevich, Sov. Phys. JETP **2**, 636 (1956).  
 [6] N. P. Armitage, E. J. Mele, and A. Vishwanath, *Rev. Mod. Phys.* **90**, 015001 (2018).  
 [7] G. P. Mikitik and Y. V. Sharlai, *Phys. Rev. Lett.* **82**, 2147 (1999).  
 [8] A. Alexandradinata and L. Glazman, *Phys. Rev. Lett.* **119**, 256601 (2017).

[9] A. Alexandradinata and L. Glazman, *Phys. Rev. B* **97**, 144422 (2018).  
 [10] A. Balatskii, G. Volovik, and A. Konyshev, Zh. Eksp. Teor. Fiz. **90**, 2038 (1986).  
 [11] C.-L. Zhang *et al.*, *Nat. Phys.* **13**, 979 (2017).  
 [12] C.-K. Chan and P. A. Lee, *Phys. Rev. B* **96**, 195143 (2017).  
 [13] G. Bednik, K. S. Tikhonov, and S. V. Syzranov, *Phys. Rev. Research* **2**, 023124 (2020).  
 [14] C. M. Wang, H.-Z. Lu, and X. C. Xie, *Phys. Rev. B* **102**, 041204(R) (2020).  
 [15] A. C. Potter, I. Kimchi, and A. Vishwanath, *Nat. Commun.* **5**, 5161 (2014).  
 [16] J. Knolle and N. R. Cooper, *Phys. Rev. Lett.* **115**, 146401 (2015).  
 [17] J. Knolle and N. R. Cooper, *Phys. Rev. Lett.* **118**, 176801 (2017).  
 [18] L. Zhang, X.-Y. Song, and F. Wang, *Phys. Rev. Lett.* **116**, 046404 (2016).  
 [19] H. K. Pal, F. Piéchon, J.-N. Fuchs, M. Goerbig, and G. Montambaux, *Phys. Rev. B* **94**, 125140 (2016).  
 [20] H. K. Pal, *Phys. Rev. B* **96**, 235121 (2017).  
 [21] P. Ram and B. Kumar, *Phys. Rev. B* **96**, 075115 (2017).  
 [22] P. Ram and B. Kumar, *Phys. Rev. B* **99**, 235130 (2019).  
 [23] S. Grubinskas and L. Fritz, *Phys. Rev. B* **97**, 115202 (2018).  
 [24] H. Shen and L. Fu, *Phys. Rev. Lett.* **121**, 026403 (2018).  
 [25] Y.-W. Lu, P.-H. Chou, C.-H. Chung, T.-K. Lee, and C.-Y. Mou, *Phys. Rev. B* **101**, 115102 (2020).  
 [26] L. A. Falkovsky, *Low Temp. Phys.* **37**, 815 (2011).  
 [27] Z. Z. Alisultanov, *JETP Lett.* **104**, 188 (2016).  
 [28] See Supplemental Material at <http://link.aps.org/supplemental/10.1103/PhysRevLett.127.116602> for additional details of the theoretical analysis, including (i) various analytic properties of the exact solution, (ii) TCI surface state exact solution, (iii) mapping to the Rabi model, (iv) a tight-binding model realization, (v) details regarding Weyl semimetal conductivity calculations, and (vi) details of the non-LK temperature dependence, which includes Refs. [29–31].  
 [29] F. D. M. Haldane, *Phys. Rev. Lett.* **61**, 2015 (1988).  
 [30] C. L. Kane and E. J. Mele, *Phys. Rev. Lett.* **95**, 226801 (2005).  
 [31] DLMF, *NIST Digital Library of Mathematical Functions*, edited by F. W. J. Olver, A. B. Olde Daalhuis, D. W. Lozier, B. I. Schneider, R. F. Boisvert, C. W. Clark, B. R. Miller, B. V. Saunders, H. S. Cohl, and M. A. McClain.  
 [32] A. V. Turbiner, *Commun. Math. Phys.* **118**, 467 (1988).  
 [33] D. Braak, *Phys. Rev. Lett.* **107**, 100401 (2011).  
 [34] Q. Xie, H. Zhong, M. T. Batchelor, and C. Lee, *J. Phys. A* **50**, 113001 (2017).  
 [35] L. Fu, *Phys. Rev. Lett.* **106**, 106802 (2011).  
 [36] J. Liu, W. Duan, and L. Fu, *Phys. Rev. B* **88**, 241303(R) (2013).  
 [37] Reference [38] observed (but did not discuss) ZQOs in this system.  
 [38] M. Serbyn and L. Fu, *Phys. Rev. B* **90**, 035402 (2014).  
 [39] T. H. Hsieh, H. Lin, J. Liu, W. Duan, A. Bansil, and L. Fu, *Nat. Commun.* **3**, 982 (2012).  
 [40] Y. Okada, M. Serbyn, H. Lin, D. Walkup, W. Zhou, C. Dhital, M. Neupane, S. Xu, Y. J. Wang, R. Sankar, F. Chou,

- A. Bansil, M. Z. Hasan, S. D. Wilson, L. Fu, and V. Madhavan, *Science* **341**, 1496 (2013).
- [41] Y. J. Wang, W.-F. Tsai, H. Lin, S.-Y. Xu, M. Neupane, M. Z. Hasan, and A. Bansil, *Phys. Rev. B* **87**, 235317 (2013).
- [42] B. Assaf, T. Phuphachong, V. Volobuev, A. Inhofer, G. Bauer, G. Springholz, L. de Vaulchier, and Y. Guldner, *Sci. Rep.* **6**, 20323 (2016).
- [43] S. E. Sebastian and C. Proust, *Annu. Rev. Condens. Matter Phys.* **6**, 411 (2015).
- [44] Y.-H. Chan, C.-K. Chiu, M. Y. Chou, and A. P. Schnyder, *Phys. Rev. B* **93**, 205132 (2016).
- [45] C. Fang, H. Weng, X. Dai, and Z. Fang, *Chin. Phys. B* **25**, 117106 (2016).
- [46] D. T. Son and B. Z. Spivak, *Phys. Rev. B* **88**, 104412 (2013).
- [47] S. A. Parameswaran, T. Grover, D. A. Abanin, D. A. Pesin, and A. Vishwanath, *Phys. Rev. X* **4**, 031035 (2014).
- [48] Y. Baum, E. Berg, S. A. Parameswaran, and A. Stern, *Phys. Rev. X* **5**, 041046 (2015).
- [49] P. Hosur and X. Qi, *C. R. Phys.* **14**, 857 (2013).
- [50] C. W. Groth, M. Wimmer, A. R. Akhmerov, and X. Waintal, *New J. Phys.* **16**, 063065 (2014).
- [51] R. Rajaraman, *Solitons and Instantons* (North-Holland Publishing Company, Amsterdam, 1982).
- [52] J. K. Jain and S. Kivelson, *Phys. Rev. A* **36**, 3467 (1987).
- [53] J. K. Jain and S. Kivelson, *Phys. Rev. B* **37**, 4111 (1988).
- [54] T. Sharpee, M. I. Dykman, and P. M. Platzman, *Phys. Rev. A* **65**, 032122 (2002).
- [55] D. Loss, D. P. DiVincenzo, and G. Grinstein, *Phys. Rev. Lett.* **69**, 3232 (1992).
- [56] J. von Delft and C. L. Henley, *Phys. Rev. Lett.* **69**, 3236 (1992).
- [57] C.-S. Park and D. K. Park, *Mod. Phys. Lett. B* **14**, 919 (2000).
- [58] U. D. Jentschura and J. Zinn-Justin, *Phys. Lett. B* **596**, 138 (2004).
- [59] G. V. Dunne and M. Ünsal, *Phys. Rev. D* **89**, 105009 (2014).
- [60] D. Dorigoni, *Ann. Phys. (Amsterdam)* **409**, 167914 (2019).
- [61] G. V. Dunne and M. Ünsal, *Annu. Rev. Nucl. Part. Sci.* **66**, 245 (2016).